

Detection of Lung Cancer Using Optimal Hybrid Segmentation and Classification

Roopa Chandrika R¹, Dr.V.Anitha², Nihar Ranjan Behera³, Dr. P. Vamsi Krishna⁴, Dr. Ravindra NamdeoraoJogekar⁵, Dr. Kamlesh Singh⁶.

¹ Associate Professor, Department of CSE, Malla Reddy College of Engineering and Technology, Hyderabad, Telangana, India,^{1*} roopachandrikaphd@yahoo.com

² Professor, Department of Computer Science and Engineering, Iyamam College of Engineering, Kannanur, Thuraiyur, Trichy, Tamilnadu, India, anitha.v81@gmail.com

³ Doctoral Researcher, Swiss School of Business and Management Geneva, Av. des Morgines 12, 1213 Petit-Lancy, Switzerland, nihar1773@gmail.com

⁴ Assistant Professor, School of Management, Malla Reddy University, Hyderabad, Telangana, India, vamsi.pratapa@yahoo.co.in

⁵ Assistant Professor, Department of Computer Science and Engineering, Priyadarshini J L College of Engineering, Nagpur, Maharashtra, India, ravindra.jogekar79@gmail.com

⁶ Professor, Department of Computer Science and Engineering, Graphic Era Hill University, Dehradun Campus, Dehradun, India, mailkamleshsingh@gmail.com

Abstract: Recently, the world health organization (WHO) showed that the lung tumor is the major leading cause of mortality. Segmentation of lung tumor is one of the exciting field for the efficient detection of lung cancer. Computerized tomography (CT) scans are used for finding the tumor position and find the cancer level in the body. This work introduces an automated diagnosis model for increasing the survival rate of patients. This work undergoes the major stages like pre-processing, hybrid segmentation, feature extraction and classification. The artifacts in the input CT images are pre-processed using noise removal technique. Then, the pre-processed image is subjected to the segmentation process. Here, the segmentation is carried out by Hybrid optimal clustering and improved region growing algorithm (IRGA). Hybrid optimal clustering is the integration of fuzzy C means clustering (FCM) and the optimization Harris Hawk algorithm (HHA). Finally, the deep features from the CT lung images are extracted and classified by the deep learning (DL) model squeezeNet. The proposed model is tested on the benchmark dataset Early Lung Cancer Action Program (ELCAP) and achieved better accuracy and specificity of 0.996 and 0.992 respectively.

Keywords: Lung Tumour, Segmentation, Optimal Clustering, CT Lung Images, Deep Learning, Classification

I. Introduction

Lung tumor is considered as one of the general diseases among human beings and it increases the mortality growth. The survival rate of the patient is enhanced by lung cancer detection at the initial stage [1]. Based on the report of the International Agency of Research on Cancer (IARC), there are 37 types of cancers and it is proven that lung tumor rate is higher in men due to their smoking habit [2]. Approximately, 2.1 million deaths occur due to cancer among these 20.14% of the deaths are caused due to lung tumor. These tumors develop in different places within the tissue of the lung [3-5].

Based on the report of the world health organization (WHO), it is found that the ratio of lung cancer ratio is increasing highly during the last six years. Generally, the lung tumor is identified manually by the symptoms of the disease like weight loss, change in voice, chest pain, memory loss and blood coughing. When these symptoms are found, various screening processes like blood tests, biopsy, genetic test and reflex tests are utilized for evaluation [6-8]. These screening techniques analyze the lung cells and variations in the cells are used for predicting the lung tumor. However, the accuracy in prediction is complex to attain [9].

Analysis of medical images plays a major role in the area of the healthcare sector particularly in

medical examination and non-invasive treatment. The medical image modalities like CT, ultrasound, X-rays and MRI images are utilized for the diagnosis. Among all screening techniques CT (computerized tomography) is one of the efficient screening modalities and it is used for examine the deviations in the parts of the body [10-12]. It is done by allowing X-rays on the body. Thirty minutes allowing of X rays analyzes the internal functions successfully. With these CT images, an automated lung tumor prediction model is generated for detecting the disease using the stages like removal of noise, segmentation of region, feature extraction, selection and classification [13].

In recent times, the computer aided diagnosis (CAD) is considered as a promising solution to assist medical experts and radiologists in diagnosing the cancer. Although different models were introduced for detecting the lung cancer, an accurate detection of the cancer remains as a challenge. The manual analysis within the tumor, and the heterogeneity of tumors made the segmentation process as complex. Several analysis are carried out for the classification of lung cancer. Some of the classical Machine learning (ML) models utilized are SVM (support vector machine), KNN (K-nearest neighbour) and ANN (artificial neural networks) [14-15]. However, these models require handcrafted feature and it leads to consume more time for the entire process. On the other hand, deep learning (DL) models are more robust in the extraction of features and classifying various stages of cancer [16-17]. The major contributions of this work are:

- To present a new noise removal technique for removing salt and pepper noise from the input CT images.
- To present hybrid segmentation based on optimal clustering and improved region growing algorithm (IRGA) for segmenting the tumor.
- To carry out classification of lung nodules using the SqueezeNet based deep learning model and compare the performance on the benchmark data.

The work is arranged as: Section 2 is about some of literature works based on lung tumor segmentation and classification. Section 3 presents the structure of the developed lung tumor model is explained in detail. Section 4 illustrates the performance measures, dataset detail and elaborated results. The entire process is concluded in Section 5.

II. Related works

Some of the recent literature works based on lung tumor segmentation and classification are listed below:

Kasinathan et al. [18] presented an automated 3D lung tumor diagnosis model using CNN and active contour method (ACM). Initially, the mediastinum and thoracic were removed and ACM was utilized for the segmentation of tumor part. Finally, an enhanced CNN model was used for classification. This model achieved better specificity and accuracy of 91% and 97% on the LIDC-IDRI dataset. Shakeel et al. [19] presented an automated lung tumor detection model using CT images. Initially, multi-level brightness preserving model was used for enhancing the image quality and eliminating the noise. The tumor regions were segmented using an enhanced deep neural network (EDNN). Then, the lung features were extracted and selected. Finally, the classification was carried out by an ensemble classifier. This model achieved better recall and precision of 0.98 and 0.974.

Neal Joshua et al. [20] demonstrated 3D-CNN and visual insights for lung tumor detection using GWCA (Gradient Weighted Class Activation). Here, the binary classification was carried out on CT images of the LUNA-16 dataset. The experimentation was carried out for tenfold cross validation and achieved better accuracy of 97.1%. Shanthi and Rajkumar [21] presented the prediction of lung cancer using SDS (stochastic diffusion approach) and the ML model. This work considered 140 (normal) and 130 (abnormal) images and the features were extracted by gabor filtering and GLCM (gray level co-occurrence matrix). Then the features were selected by SDS. The experimental analysis proved that the model based on SDN with ANN achieved a better classification accuracy of 89.6%.

Maleki et al. [22] presented KNN (K nearest neighbour) for lung tumor prognosis. Genetic algorithm (GA) was used for selecting the features and for reducing the dimensions of data. For enhancing the accuracy, the best range for k was declared by the experimentation. Meraj et al. [23] presented a lung tumor detection by semantic segmentation and classification by the optimal features. Initially, noise removal and filtering processes were carried out on pre-processing. Then, for segmenting the tumor semantic segmentation and OTSU were carried out. Then, thirteen features were extracted by PCA (principal component analysis). Among them, four features were used for classification using nine classifier. The classifiers logic boost achieved better accuracy of 99.2% on LIDC-IDRI dataset.

Yamunadevi and Siva Ranjani [24] presented lung carcinoma segmentation using adaptive fuzzy based GLCM (AF-GLCM). Here, the classification was carried out by GoogLeNet CNN and it was used for finding the cancer region was benign or malignant. Here, the experimentation was carried

out on bronchopoc images and achieved better accuracy of 97.2% (benign) and 96.1% (malignant). Marentakis et al. [25] presented a classification of lung cancer histology using radiomics and DL models. Initially, the data was collected from 102 patients and the radiomics with classifiers like KNN and SVM were used. Then, the DL models like CNN with TL (transfer learning) and three fine-tuning models were used. The performance was carried by varying the k value and spatial pooling.

III. Proposed methodology

The introduced optimization based lung tumor diagnosis model using CT images undergoes the following stages: (a) Pre-processing stage includes noise removal, extraction of background and thorax, (b) Tumor region segmentation using Hybrid optimal clustering and improved region growing algorithm (IRGA). Finally, for extracting and classification of the tumor, the DLsqueezenet model is utilized. Figure 1 presents the various phases of the proposed lung cancer segmentation and classification model.

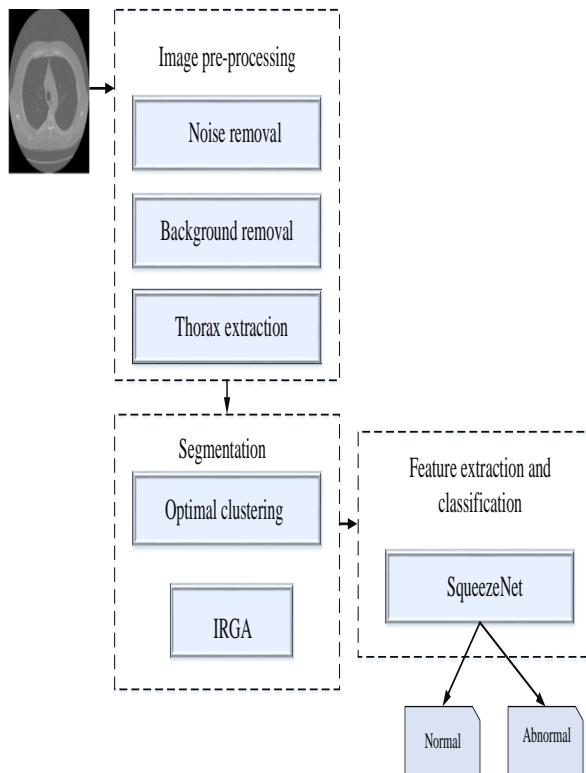


Figure 1: Proposed lung cancer segmentation and classification model

3.1 Pre-processing: It is the major process in diagnosis of the lung tumor and it undergoes the stages like noise removal, extraction of background and thorax.

Noise removal: There are two stage are involved in the removal of noise; detection and removal of noise.

Initially, the noise is detected using the Equation (1):

$$M(a,b) = \begin{cases} 1, & \text{when } \beta(a,b) \text{ noisy} \\ 0 & \text{when } \beta(a,b) \text{ noise-free} \end{cases} \quad (1)$$

where $\beta(a,b)$ and $M(a,b)$ are the input image and image with noise. In the noise detection phase, the value of maximum intensity is 255 and it is the salt noise and value of minimum intensity is 0 and it is the pepper noise. Other than this range are pixels with noise free.

Then in the noise removal stage, the initial size of the window is $[3 \times 3]$. The chosen pixel is analysed whether it is noisy or not. When the pixel doesn't have noise, the pixel is considered for further processing. If it is noise means, the values of window pixels are sorted in chronological order and saved. The nearby pixel is verified and split into categories. The first category is L and when the size of L is odd value, consider the median of

L and provided into \vec{L} . The procedure is repeated till the pixel becomes noise free. The size of the window is increased to 5 to 7 and finally, the obtained image is set as the noise removal image.

Extraction of background and thorax: After removing the noise, the thorax is extracted for segmenting the thorax from the background. Here, the grey scale thresholding is used for extracting the thorax.

3.2 Lung region segmentation: After extracting the thorax, the lung region is segmented. The major novelty of the work is the integration of Hybrid optimal clustering and IRGA for the segmentation of lung region. The segmentation processes like Otsu thresholding and morphological operations are performed; the Otsu model segment the unnecessary region since it is carried out on the basis of intensity. The morphological operation may distort the shape and the trachea is joined with the lungs. Hence, in this work Hybrid optimal clustering and IRGA.

3.2.1 FCM clustering: This model starts with initializing the cluster centers and it assigns values of membership to every data in the image pixel.

The FCM model minimizes the O_l objective function and it is given as:

$$O_l = \sum_{m=1}^N \sum_{n=1}^c u_{mn}^l \|v_m - y_n\|^2 \tag{2}$$

where l is the positive number, v_m is the i^{th} data point, u_{mn} is the membership degree of v_m in the cluster n and y_n is the centroid of cluster n . Initialize the matrix of data $U = [u_{mn}]$ and compute the vectors of centroid for the j^{th} iteration is given as:

$$Y_n = \frac{\sum_{m=1}^N u_{mn}^l v_m}{\sum_{m=1}^N u_{mn}^l} \tag{3}$$

Calculate the value of membership using the below expression:

$$u_{mn}^l = \frac{1}{\sum_{n=1}^c \left(\frac{\|v_m - y_n\|}{\|v_m - y_o\|} \right)^{2/l-1}} \tag{4}$$

At last, the minimization of O_l is given as:

$$\|O^{(t)} - O^{(t+1)}\| < \epsilon \tag{5}$$

where ϵ is the stopping term and t is the iteration.

3.2.2 HHA (Harris Hawk algorithm):This optimization [27] is based on the swarm and it is developed on the basis of the interactive characteristic of Harris Hawk during prey catching. This optimization has two phases like initialization phase and updation phase. The initialization phase is used for determining the initial parameters for HHA. The updation phase carries out exploration and exploitation processes.

Exploration: In this process, the search agents search different fields for exploring the prey location. It is expressed as:

$$Z(t+1) = \begin{cases} Z_r(t) - rand1 | Z_r(t) - 2rand2 \times Z(t) & p \geq 0.5 \\ Z_{target}(t) - Z_{avg}(t) - rand3 \times (rand4(UL - LL) + LL) & p < 0.5 \end{cases} \tag{6}$$

where $Z(t+1)$ and $Z(t)$ are the position vectors of Harris hawks at the iterations $t+1$ and t .

$rand1, rand2, rand3, rand4$ and p are the random values. $Z_r(t), Z_{target}(t)$ and $Z_{avg}(t)$ are the position vectors of the random search agent, rabbit and average position.

Moving from exploration to exploitation: The balancing among these two processes in HHA is on the basis of energy of prey. This energy minimizes on the escaping and it is given as:

$$Esc.energy = 2E_0 \left(1 - \frac{t}{T} \right) \tag{7}$$

where T is the maximum iteration and E_0 is the initial state.

Exploitation: In this process, the search agents control exploitation. When the prey escapes or not, the hawks select the besieging prey on the basis of energy of the prey. Here, E is used for controlling the changes between soft besiege (SB) and hard besiege (HB). The SB is carried out during $Esc.energy \geq 0.5$ and HB is carried out during $Esc.energy < 0.5$. In SB, $Esc.energy \geq 0.5$ and $r \geq 0.5$, the Harris hawks tries to round the best search agent and it is given as:

$$Z(t+1) = \Delta Z(t) - Esc.energy | jump\ strength \times Z_{target}(t) \tag{8}$$

where $\Delta Z(t)$ is the variation among the best agent position and present location and $jump\ strength$ is the jumping capacity of rabbit. Then the best agent position in HB is given as:

$$Z(t+1) = Z_{target}(t) - Esc.energy \times |\Delta Z(t)| \tag{9}$$

The above two processes are carried out when $r \geq 0.5$. When $r < 0.5$, both SB and HB are carried out by motion of fast dives.

When $Esc.energy \geq 0.5$ and $r < 0.5$, the next movements are generated on the basis of the following expression:

$$X = Y + R \times Levy(Dim) \tag{11}$$

The Levy's flight is utilized for calculating the fast dives and it is given as:

where R and Dim are the random vector and dimension. here, the current agent's position is updated by:

$$Z(t+1) = \begin{cases} Y & \text{when } F(Y) < Z(t) \\ X & \text{when } F(X) < X(t) \end{cases} \quad (12)$$

Finally, when $Esc.energy < 0.5$ and $r < 0.5$, the search agents attempt to remove the variation of mean location and intended prey. The present location is carried out on the basis of following two expressions:

$$Y' = Z_{target}(t) - Esc.energy \times |jump\ strength \times Z| \quad (13)$$

$$X' = Y' + R \times Levy(Dim) \quad (14)$$

Hence, the present location is written as:

$$Z(t+1) = \begin{cases} Y' & \text{when } F(Y') < Z(t) \\ X' & \text{when } F(X') < X(t) \end{cases} \quad (15)$$

3.2.3 Optimal clustering (FCM-HHA): In this work, FCM is hybrid with HHA for obtaining best cluster with minimal cost. HHA is used for finding the optimal solution. FCM is given on the data points for obtaining the initial clusters and HHA is utilized on the obtained clusters for optimizing the position of the cluster center. In the optimization process, every cluster is initialized as the population of Harris hawks. Algorithm 1 shows the pseudocode of FCM-HHA.

<p>Algorithm 1: Pseudocode of FCM-HHA Input: Clusters, size of population and maximum number of iterations Output: Optimal cluster center Carry out FCM on the Lung images Arrange the data on the basis of clusters C_1, C_2, \dots, C_l For every cluster 1 to l Compute the cost function for every Harris hawks Define the best Z_{target} end for Update $Esc.energy$ on the basis of Equation (7) When $Esc.energy \geq 1$ Current agent's position is updated on the basis of Equation (6) when $Esc.energy \geq 0.5$ and $r \geq 0.5$ Current agent's position is updated on the basis of Equation (8) Endif when $Esc.energy < 0.5$ and $r \geq 0.5$ Current agent's position is updated on the basis of Equation (9) Endif when $Esc.energy \geq 0.5$ and $r < 0.5$ Current agent's position is updated on the basis of Equation (12) when $Esc.energy < 0.5$ and $r < 0.5$ Current agent's position is updated on the basis of Equation (13) endif end for $t = t + 1$ Return the best Z_{target} Again carry out FCM with best cluster centers</p>
--

3.2.4 Improved region growing algorithm (IRGA):

This algorithm uses pixels in similar region that have the same features. Here, the initial seed points are selected at the pixel on the lung region not on the tumor region. In the normal RGA, noise inclusion and intensity variation values may attain over segmentation. Hence, in this work IRGA is introduced for overcoming the drawbacks of RGA. Here, the criteria orientation is included and two threshold values are set. Then, the region growing is developed by the neighbouring pixels which satisfy both the threshold values. The process of IRGA is given below:

- Initialize the gradient values at x axis $I(X)$ and y axis $I(Y)$.
- Identify the gradient vectors by combining the gradients on x and y axis.
- The following expression is used for finding the gradient vector

$$G(X, Y) = \left(\frac{1}{1 + (I(X)^2 + (Y)^2)} \right) \quad (16)$$

- The $G(X, Y)$ is converted from radians to degree and the images are split in grid $g(j)$.
- Define the thresholds of intensity and orientation as Th_I and Th_O .
- For every grid $g(j)$,
 - A histogram is created for each pixel in a grid $g(j)$.
 - Estimate the histogram which occurs frequently $k(H)$.
 - Choose any one of the histograms as the seed point having intensity and orientation as $k_{(I)}$ and $k_{(O)}$
 - Verify criteria
 1. The criteria of intensity is $\|k_{(I)} - Neighbour_{(I)}\|$.
 2. The criteria of orientation is $\|k_{(O)} - Neighbour_{(O)}\|$.
- When the neighbouring pixel having intensity $Neighbour_{(I)}$ and orientation $Neighbour_{(O)}$ satisfied the above criteria.
- The region develops to the neighbouring pixel.

3.3 Feature extraction and classification

The deep learning (DL) model SqueezeNet is used for extracting and classifying the nodules. This network is used for classifying the tumor as benign or malignant. This network has 18 layers of a deep convolutional network and it is composed of less number of parameters and manages better accuracy. Figure 2 shows the structure of pre-trained SqueezeNet. This network starts with one conv1 (convolutional layer), 8 fire modules (Fire 2 to Fire 9) and ends with one conv10 (convolutional layer). For every layer, total filters per Fire module are improved. This network carries out maxpooling with 2 strides after the layers of conv1 to conv10.

Pre-trained model exploits transfer learning (TL) for improving the performance of the tumor classification. TL reduces the total training data required particularly in healthcare applications. Fine-tuning is the process of slightly altering the present FC (fully connected) layers of the classifier and particular layers of CNN. In this work, the pre-

trained model used in VGG19. cross entropy (CE) is the loss function utilized and it is given as:

$$L_{CE} = -\sum_{k=1}^M a^{(k)} \log b^{(k)} \quad (17)$$

where M is the total samples, $a^{(k)}$ and $b^{(k)}$ are the true and predicted labels at the k^{th} class. Finally, the SqueezeNet classifies the results as 0 (normal) and 1 (abnormal).

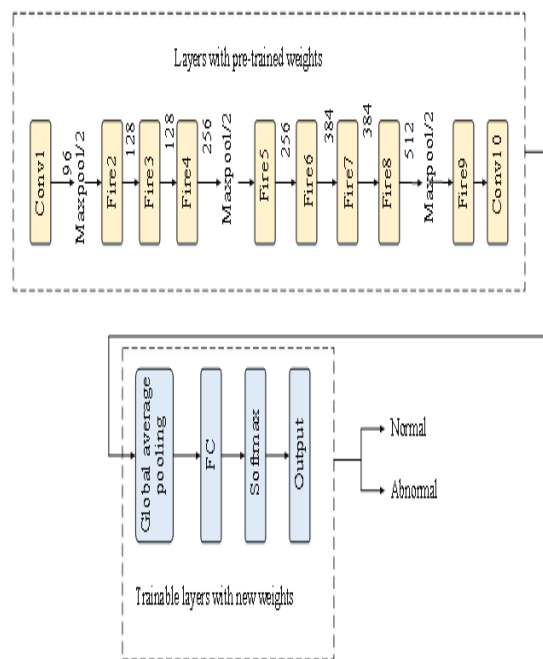


Figure 2: Structure of pre-trained SqueezeNet

IV. Results analysis

The following section shows the performance of the proposed segmentation and classification of the lung tumor. The entire simulation is carried out in Python 3.7 platform and Intel core i3 processor with 16 GB RAM. Table 1 shows the hyperparameters used for the experimentation.

Table 1: Hyperparameters and its values

Hyperparameters	values
Kernels size	(3,3) , (1,1)
Activation function	Relu
Pooling size	(2,2) , (3,3)
Dropout ratio	0.1
loss	CE
optimizer	Adam
Epoch	100
Batch size	32

4.2 Dataset details

In this work, the dataset used in ELCAP [26] is considered; this dataset has fifty low dose CT lung images having 1.25mm thickness. The nodule locations identified by the radiologists are given.

This site ensures a group of interactive image viewer tools for the CT images as well as the annotations. The sample images of this dataset are given in Figure 3.

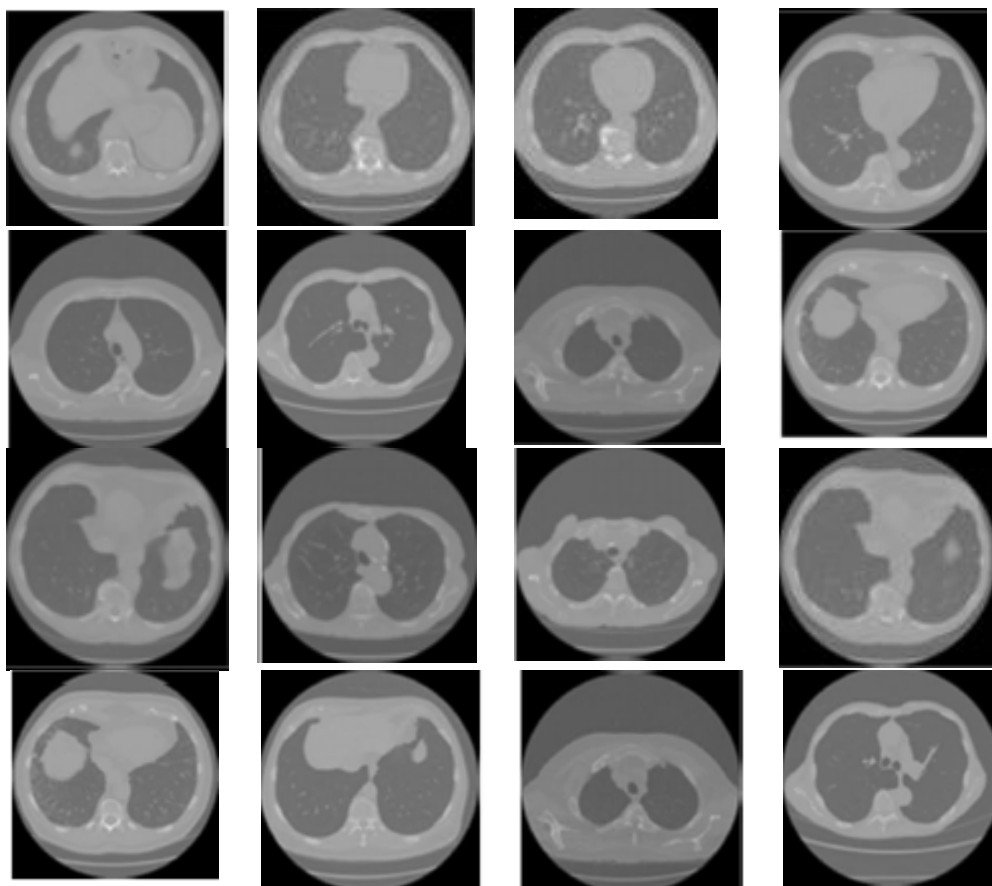


Figure 3: Sample images of the ELCAP dataset

4.3 Performance metrics

The robustness of proposed lung tumor segmentation and classification is analyzed quantitatively by the measures like accuracy, precision, Recall, IOU (Intersection over Union) and dice score, Mathews correlation coefficient (MCC) confusion matrix (CM) and receiver operating characteristic curve (ROC). These measures are measured by true positive T_p , is the ratio of the patient with a lung tumor is identified as having a lung tumor, False negative F_p is ratio of the identified value for the normal people is identified as having lung tumor, true negative T_n is ratio of the affected people with lung tumor identified as healthy and False negative F_n is the normal people is identified as cancer affected patient. Table 2 shows the metrics with their expressions.

Table 2: Metrics with their expressions

Metric s	Formula
Accuracy	$Acc = \frac{T_p + T_n}{T_p + T_n + F_p + F_n}$
Precision	$P = \frac{T_p}{T_p + F_p}$
Recall	$R = \frac{T_p}{T_p + F_n}$
mIOU	$mIOU = \frac{1}{n} \sum_{i=1}^n \frac{T_p + T_n}{T_p + T_n + F_p + F_n}$
Dice	$Dice = \frac{2T_p}{2T_p + F_p + F_n}$

4.3 Qualitative analysis

The qualitative analysis of the proposed diagnosis model of three images is presented in Figure 4. In the Figure, the first row shows the input CT image, then the filtered image, background removal and thorax extracted images. Then, the second row shows the segmented images of optimal clustering and IRGA images. Finally, the extracted nodule is given in Figure 4.

The utilization of optimal clustering is essential since the lung and tumor present in the input images have a fuzzy boundary. Hence, optimal clustering finds all fine tumors in the lungs. Further, IRGW is essential in eliminating the redundant parts attained from the clustering. Then, the SqueezeNet extracted and classified the tumor which is shown in the final image.

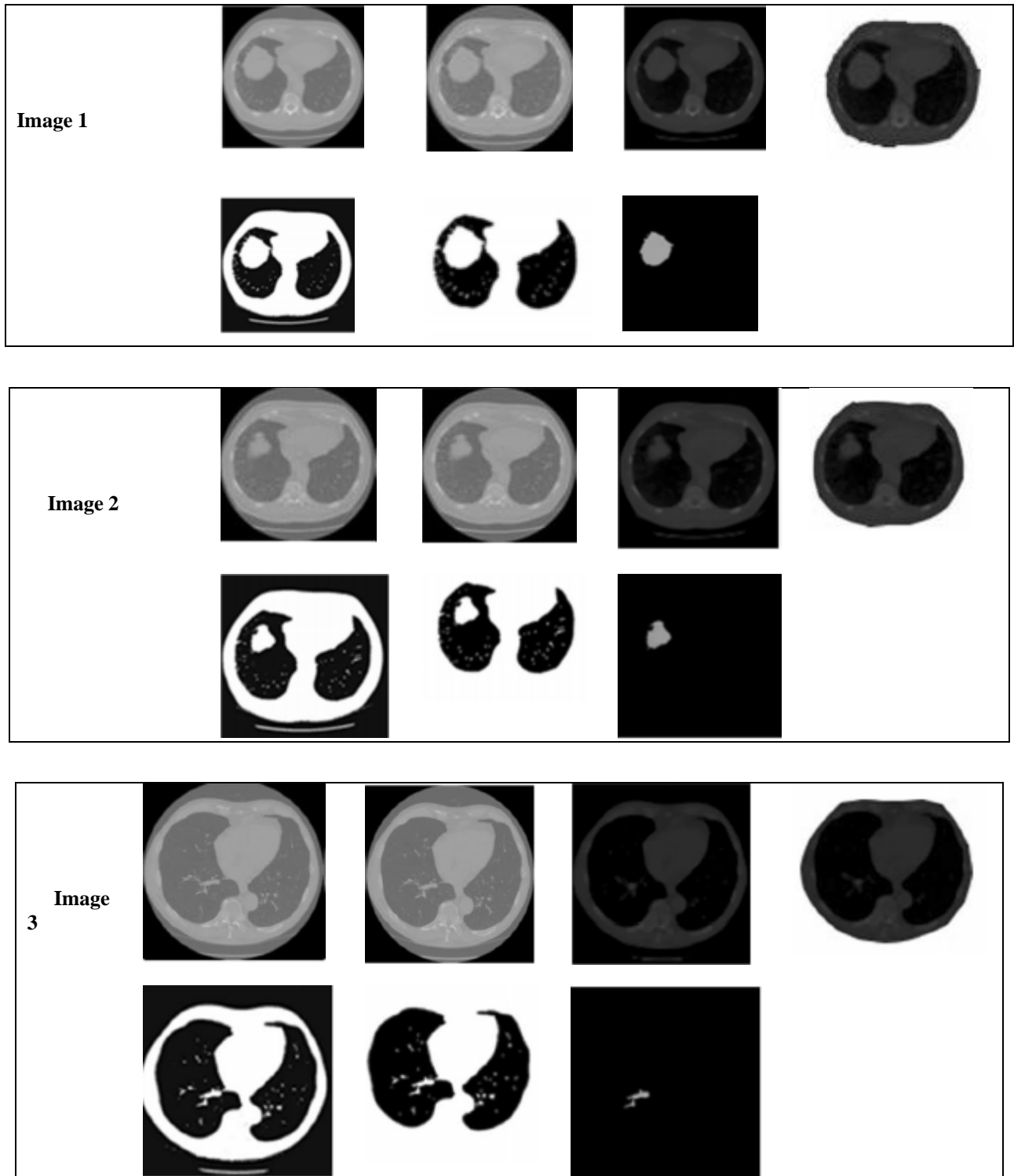


Figure 4: Qualitative analysis of the proposed model

Table 3 presents the performance comparison of various segmentation models. The algorithms like FCM, Region growing, OTSU, Optimal clustering, and IPGA are compared with the proposed segmentation. When comparing the performance of all algorithms it is found that the proposed model achieved better segmentation accuracy, mIOU and Dice values of 0.996, 0.978 and 0.988 respectively. The proposed model achieved better results because of optimal cluster selection and IRGA. Thus it is proved that proposed segmentation and classification model efficiently segmented and classified the lung tumor.

Table 3: Performance comparison of various segmentation models

Methods	Accuracy	Precision	Recall	mIOU	Dice
FCM	0.783	0.789	0.821	0.783	0.804
Region growing	0.786	0.803	0.834	0.792	0.837
OTSU	0.801	0.823	0.812	0.835	0.867
Optimal clustering	0.845	0.872	0.845	0.846	0.953
IPGA	0.856	0.945	0.973	0.956	0.967
proposed	0.996	0.986	0.992	0.978	0.988

Figure 5 delineates the accuracy and loss curves of the proposed SqueezeNet model on the ELCAP dataset. Here, the performance is carried out by varying the epoch value from 0 to 150 iterations. In this graph, x-axis is the total training cycles and y-axis is the loss and accuracy. It is observed from the accuracy graph that the in the initial stage, testing accuracy is higher than the testing accuracy for some value of epoch. When the epoch is increased, the accuracy is also increased.

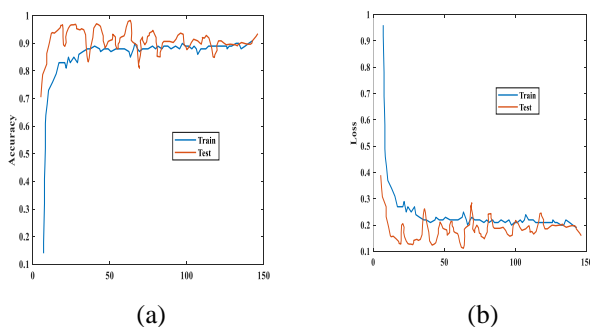


Figure 5: Accuracy and loss curves of the SqueezeNet model

Practically, the classification of medical data is more sensitive and the evaluating all classifiers are needed for comparing their sensitivity and specificity with the entire frequency, Figure 6 shows the CM of the SqueezeNet model and it is plotted for the actual and predicted values. From the CM it is found that the accuracy of classification is 99%, sensitivity is 100% and specificity is 98%. Further, only one abnormal image is incorrectly identified by the SqueezeNet model.

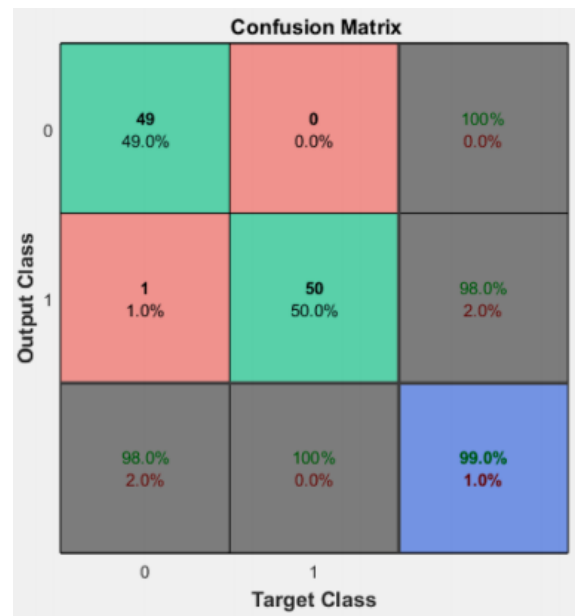


Figure 6: CM of the SqueezeNet model

The accuracy of the classification is estimated using the ROC curve and it is plotted with respect to TPR (true positive rate) and false positive rate (FPR). It is plotted by setting the threshold value. TRP is the recall value and FPR is the fallout. That is the curve is plotted for recall and fallout values of the classifier. The fallout is computed using subtracting one from the recall value. Here, 0 indicates the normal and 1 is the abnormal cases. It is observed from Figure 7 that the AUC (area under the curve) value achieved is almost 100% for all the values of the FPR.

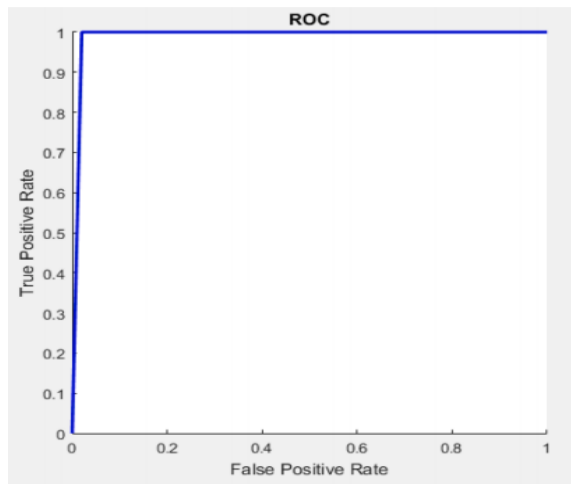


Figure 7: ROC curve of the SqueezeNet model

V. Conclusion

This work presents a lung cancer classification model using the deep learning (DL). The hybrid segmentation model was developed for accurately segmenting the tumor. Optimal clustering was carried out by FCM-HHA and then orientation based RGA (IRGA) to efficiently segment the tumor. Further, the DL model SqueezeNet model was used for classifying the nodules. From the experimental outcomes, it was found that the proposed hybrid segmentation detected tumor of various sizes and shapes correctly. The performance was carried out on the ELCAP dataset and various performance metrics were carried out. Finally, it was proved that the proposed model achieved segmentation and classification performance when compared to other algorithms. In the future, we will provide the enhanced DL model for the segmentation of tumors. Further, we will enhance the model for various modalities of lung tumor images.

References

- [1] Maqsood, M., Yasmin, S., Mehmood, I., Bukhari, M. and Kim, M., 2021. An efficient DAnet architecture for lung nodule segmentation. *Mathematics*, 9(13), p.1457.
- [2] Pezzano, G., Ripoll, V.R. and Radeva, P., 2021. CoLe-CNN: Context-learning convolutional neural network with adaptive loss function for lung nodule segmentation. *Computer Methods and Programs in Biomedicine*, 198, p.105792.
- [3] Priya, R.M. and Venkatesan, P., 2021. An efficient image segmentation and classification of lung lesions in pet and CT image fusion using DTWT incorporated SVM. *Microprocessors and Microsystems*, 82, p.103958.
- [4] Han, Y., Ma, Y., Wu, Z., Zhang, F., Zheng, D., Liu, X., Tao, L., Liang, Z., Yang, Z., Li, X. and Huang, J., 2021. Histologic subtype classification of non-small cell lung cancer using PET/CT images. *European journal of nuclear medicine and molecular imaging*, 48(2), pp.350-360.
- [5] Li, J., Chen, H., Li, Y., Peng, Y., Cai, N. and Cao, X., 2021. AMRSegNet: adaptive modality recalibration network for lung tumor segmentation on multi-modal MR images. *Multimedia Tools and Applications*, 80(25), pp.33779-33797.
- [6] Calheiros, J.L.L., de Amorim, L.B.V., de Lima, L.L., de Lima Filho, A.F., Ferreira Júnior, J.R. and de Oliveira, M.C., 2021. The effects of perinodular features on solid lung nodule classification. *Journal of Digital Imaging*, 34(4), pp.798-810.
- [7] Chen, K.B., Xuan, Y., Lin, A.J. and Guo, S.H., 2021. Lung computed tomography image segmentation based on U-Net network fused with dilated convolution. *Computer Methods and Programs in Biomedicine*, 207, p.106170.
- [8] Nanglia, P., Kumar, S., Mahajan, A.N., Singh, P. and Rathee, D., 2021. A hybrid algorithm for lung cancer classification using SVM and Neural Networks. *ICT Express*, 7(3), pp.335-341.
- [9] Jalaldeen, K., Malathi, M., Sinthia, P., Vadivel, M. and Shankar, B.M., 2021. An automatic identification of lung tumor by using CNN network and fuzzy-clustering algorithm. *Materials Today: Proceedings*, 45, pp.2921-2924.
- [10] Gu, D., Liu, G. and Xue, Z., 2021. On the performance of lung nodule detection, segmentation and classification. *Computerized Medical Imaging and Graphics*, 89, p.101886.
- [11] Yang, J., Wu, B., Li, L., Cao, P. and Zaiane, O., 2021. MSDS-UNet: A multi-scale deeply supervised 3D U-Net for automatic segmentation of lung tumor in CT. *Computerized Medical Imaging and Graphics*, 92, p.101957.
- [12] Shakeel, P.M., Burhanuddin, M.A. and Desa, M.I., 2019. Lung cancer detection from CT image using improved profuse clustering and deep learning instantaneously trained neural networks. *Measurement*, 145, pp.702-712.
- [13] Delzell, D.A., Magnuson, S., Peter, T., Smith, M. and Smith, B.J., 2019. Machine learning and feature selection methods for disease classification with application to lung cancer screening image data. *Frontiers in oncology*, 9, p.1393.
- [14] Singh, G.A.P. and Gupta, P.K., 2019. Performance analysis of various machine learning-based approaches for detection and classification of lung cancer in humans. *Neural Computing and Applications*, 31(10), pp.6863-6877.

- [16] Kasinathan, G., Jayakumar, S., Gandomi, A.H., Ramachandran, M., Fong, S.J. and Patan, R., 2019. Automated 3-D lung tumor detection and classification by an active contour model and CNN classifier. *Expert Systems with Applications*, 134, pp.112-119.
- [17] Lakshmanaprabu, S.K., Mohanty, S.N., Shankar, K., Arunkumar, N. and Ramirez, G., 2019. Optimal deep learning model for classification of lung cancer on CT images. *Future Generation Computer Systems*, 92, pp.374-382.
- [18] Kasinathan, G., Jayakumar, S., Gandomi, A.H., Ramachandran, M., Fong, S.J. and Patan, R., 2019. Automated 3-D lung tumor detection and classification by an active contour model and CNN classifier. *Expert Systems with Applications*, 134, pp.112-119.
- [19] Shakeel, P.M., Burhanuddin, M.A. and Desa, M.I., 2020. Automatic lung cancer detection from CT image using improved deep neural network and ensemble classifier. *Neural Computing and Applications*, pp.1-14.
- [20] Neal Joshua, E.S., Bhattacharyya, D., Chakkravarthy, M. and Byun, Y.C., 2021. 3D CNN with visual insights for early detection of lung cancer using gradient-weighted class activation. *Journal of Healthcare Engineering*, 2021.
- [21] Shanthi, S. and Rajkumar, N., 2021. Lung cancer prediction using stochastic diffusion search (SDS) based feature selection and machine learning methods. *Neural Processing Letters*, 53(4), pp.2617-2630.
- [22] Maleki, N., Zeinali, Y. and Niaki, S.T.A., 2021. A k-NN method for lung cancer prognosis with the use of a genetic algorithm for feature selection. *Expert Systems with Applications*, 164, p.113981.
- [23] Meraj, T., Rauf, H.T., Zahoor, S., Hassan, A., Lali, M.I., Ali, L., Bukhari, S.A.C. and Shoaib, U., 2021. Lung nodules detection using semantic segmentation and classification with optimal features. *Neural Computing and Applications*, 33(17), pp.10737-10750.
- [24] Yamunadevi, M. M., and S. Siva Ranjani. "Efficient segmentation of the lung carcinoma by adaptive fuzzy-GLCM (AF-GLCM) with deep learning based classification." *Journal of Ambient Intelligence and Humanized Computing* 12, no. 5 (2021): 4715-4725.
- [25] Marentakis, Panagiotis, PantelisKaraiskos, Vassilis Kouloulis, Nikolaos Kelekis, Stylianos Argentos, Nikolaos Oikonomopoulos, and Constantinos Loukas. "Lung cancer histology classification from CT images based on radiomics and deep learning models." *Medical & Biological Engineering & Computing* 59, no. 1 (2021): 215-226.
- [26] Reeves, Anthony P., Alberto M. Biancardi, D. Yankelevitz, S. Fotin, Brad M. Keller, ArtitJirapatnakul, and Jaesung Lee. "A public image database to support research in computer aided diagnosis." *In 2009 Annual International Conference of the IEEE Engineering in Medicine and Biology Society*, pp. 3715-3718. IEEE, 2009.
- [27] Heidari, A.A., Mirjalili, S., Faris, H., Aljarah, I., Mafarja, M. and Chen, H., 2019. Harris hawks optimization: Algorithm and applications. *Future generation computer systems*, 97, pp.849-872.